

Online Research @ Cardiff

This is an Open Access document downloaded from ORCA, Cardiff University's institutional repository: <https://orca.cardiff.ac.uk/id/eprint/140411/>

This is the author's version of a work that was submitted to / accepted for publication.

Citation for final published version:

Li, Benxuan, Hou, Bo ORCID: <https://orcid.org/0000-0001-9918-8223> and Amaratunga, Gehan A. J. 2021. Indoor photovoltaics, the next big trend in solution-processed solar cells. InfoMat 3 (5) , pp. 445-459. 10.1002/inf2.12180 file

Publishers page: <http://dx.doi.org/10.1002/inf2.12180>
<<http://dx.doi.org/10.1002/inf2.12180>>

Please note:

Changes made as a result of publishing processes such as copy-editing, formatting and page numbers may not be reflected in this version. For the definitive version of this publication, please refer to the published source. You are advised to consult the publisher's version if you wish to cite this paper.

This version is being made available in accordance with publisher policies.

See

<http://orca.cf.ac.uk/policies.html> for usage policies. Copyright and moral rights for publications made available in ORCA are retained by the copyright holders.



REVIEW ARTICLE

Indoor photovoltaics, *The Next Big Trend* in solution-processed solar cells

Benxuan Li¹ | Bo Hou² | Gehan A. J. Amaratunga¹ 

¹Electrical Engineering Division,
Engineering Department, University of
Cambridge, Cambridge, UK

²School of Physics and Astronomy, Cardiff
University, Cardiff, Wales, UK

Correspondence

Bo Hou, School of Physics and
Astronomy, Cardiff University, Cardiff,
Wales, CF24 3AA, UK.
Email: houb6@cardiff.ac.uk

Gehan A. J. Amaratunga, Electrical
Engineering Division, Engineering
Department, University of Cambridge,
9 JJ Thomson Avenue, Cambridge, CB3
0FA, UK.
Email: gajal@cam.ac.uk

Funding information

Cardiff University, Grant/Award Number:
Grant to Bo Hou; UK Engineering and
Physical Sciences Research Council,
Grant/Award Number: EP/P027628/1

Abstract

Indoor photovoltaics (IPVs) have attracted considerable interest for their potential to power small and portable electronics and photonic devices. The recent advances in circuit design and device optimizations has led to the power required to operate electronics for the internet of things (IoT), such as distributed sensors, remote actuators, and communication devices, being remarkably reduced. Therefore, various types of sensors and a large number of nodes can be wireless or even batteryless powered by IPVs. In this review, we provide a comprehensive overview of the recent developments in IPVs. We primarily focus on third-generation solution-processed solar cell technologies, which include organic solar cells, dye-sensitized solar cells, perovskite solar cells, and newly developed colloidal quantum dot indoor solar cells. Besides, the device design principles are also discussed in relation to the unique characteristics of indoor lighting conditions. Challenges and prospects for the development of IPV are also summarized, which, hopefully, can lead to a better understanding of future IPV design as well as performance enhancement.

KEYWORDS

dye-sensitized solar cells, indoor photovoltaics, organic solar cells, perovskite solar cells, quantum dot solar cells

1 | INTRODUCTION

Energy is considered as one of the primary challenges for the sustainable development of human societies. Environmentally friendly renewable energy sources, as an alternative to conventional fossil fuels, have witnessed extensive development during past decades because of their potential to provide energy without greenhouse gas emissions and hence mitigate climate change through global warming. Among a variety of renewable energy sources, photovoltaic (PV) technologies which enable direct conversion of solar energy to electricity account for

a substantial and growing proportion of alternative energy electricity generation capacity globally. It is also attractive as it is a modular technology which in principle can be installed everywhere without geographical limitation.¹ Solution-processed PV cells form a subset and have the benefit of low cost, due to the low energy budget incurred in their fabrication. They are therefore particularly suited for PV conversion in environments which have significantly lower light intensity than that available from direct sunlight. The efficiency of energy conversion in low light environments (typically 0.01 Sun) can in fact be higher in solution-processed organic PV cells

This is an open access article under the terms of the Creative Commons Attribution License, which permits use, distribution and reproduction in any medium, provided the original work is properly cited.

© 2021 The Authors. *InfoMat* published by John Wiley & Sons Australia, Ltd on behalf of UESTC and John Wiley & Sons Australia Ltd.

compared to their inorganic counterparts which operate in direct sunlight. This class of PV has attracted considerable attention not only in terms of photovoltaic device optimization but also in materials and chemistry innovations.²⁻⁴

Because of the recent advances in circuit design and device optimizations, the power required to operate electronics for the internet of things (IoT), such as distributed sensors, remote actuators, and communication devices, has been significantly reduced. As presented in Figure 1 (A), the cost of low-power electronics has also reduced due to increasing integration and use of low-cost substrates together with low-cost manufacturing routes such as printing. To further enhance the versatility of location and applicability, deploying PV technologies into the indoor environment to realize wireless and battery-free self-powered electronic systems such as wireless sensors, radio-frequency identification (RFID) tags, and Bluetooth beacons becomes an attractive option.⁵ A significant portion of these electronic systems will form a crucial part of the IoT ecosystem, where large networks of connected devices collect and communicate data from the environment. Having long-term local energy sources for providing power to devices in such networks can be partly realized through photovoltaic conversion and capacitive storage. However, the prevalent silicon (Si) PVs generally have poor performance under ambient light conditions, are also costly when operated at much lower levels of energy conversion than the capability of Si (which is not even approached under terrestrial solar insolation) and difficult to integrate into small, lightweight, and portable systems for the IoT.⁵⁻⁷

As alternatives to Si-based PVs, the third-generation solution-processed solar cells, including dye-sensitized

solar cells (DSSCs), organic solar cells (OSCs), quantum dot solar cells (QDSCs), and perovskite solar cells (PSCs), which have made considerable progress in recent years, are a viable option. Due to their large absorption cross-section, substrate-independent processability and broad bandgap customizability, there has been extensive research on deploying these solar cells into indoor photovoltaic (IPV) applications which can be used for powering IoT-related electronics.⁸ However, it is worthwhile emphasizing that different types of third-generation PVs exhibit different drawbacks, such as poor stability, toxicity in PSCs, and photodegradation in OSCs.⁹

In this review, we first introduce the design principles for IPV since the operating conditions and power output are considerably different from solar cells designed to operate under AM1.5 (1 kW m^{-2}) insolation. Then, we summarize the recent development of IPVs from first-generation Si-based PVs to third-generation counterparts by tracking performance improvement as well as the underlying physical mechanisms. According to the property of each IPV, discussions about potential challenges that hinder their indoor application and potential solutions are presented.

2 | THE DESIGN PRINCIPLES FOR IPVs

The device working area for an IPV is only a few square centimeters, with incident light intensity as low as $0.1\text{--}10 \text{ W m}^{-2}$ mainly in the visible region from diffuse solar radiation in the indoor environment and ambient

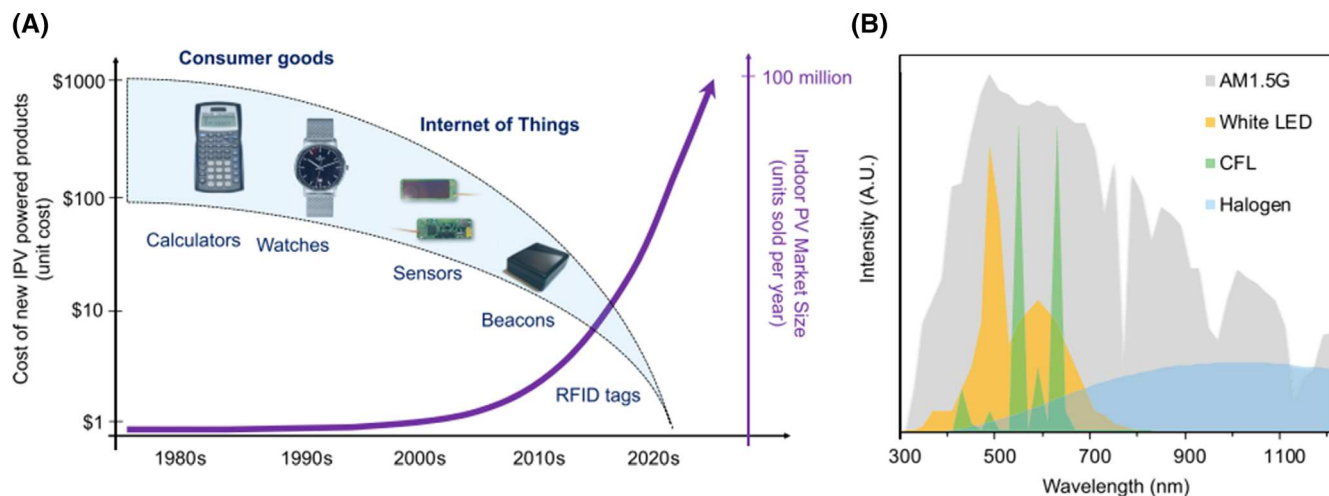


FIGURE 1 (A) An overview of the cost of indoor photovoltaic (IPV)-powered devices and the prediction of IPV market size.

(B) Different light spectra under which IPV efficiency is evaluated, including the standard solar spectrum AM1.5G and typical spectra from white light-emitting diode (LED), compact fluorescent lamps (CFL), and Halogen sources. Copyright 2019, Elsevier

artificial light sources such as incandescent light bulbs, compact fluorescent lamps, and white light-emitting diodes (LEDs).¹⁰ Indoor lighting applications are designed and optimized based on the spectral sensitivity of human eyes, which peaks at 550 nm in a range from 380 to 780 nm.¹¹ Therefore, IPV can exploit the advantage of a higher open-circuit voltage (V_{oc}) when shifting to larger bandgaps, while simultaneously benefiting from a high photon yield. For indoor lighting, lux is used as a metric of light intensity, corresponding to the spectrum responsivity of human eyes to a different wavelength. Typically, 200 lux is for living room environments and 300–2000 lux for the office or other indoor environments.^{12,13}

Changing the light source from AM 1.5G to indoor lights changes not only the intensity but also the spectrum of the incident lighting as indoor light lies only in the visible range, as shown in Figure 1(B). Therefore, optimization of IPV is sought with photoactive materials having wider bandgaps than Si. The extinction coefficient of active materials is also of great importance. Other issues include the optimization of the interfacial layers, which accounts for the charge transfer and collection.⁸

3 | THE DEVELOPMENT OF PHOTOVOLTAICS FOR INDOOR APPLICATION

3.1 | Conventional thin-film Si-based solar cells for indoor application

To date, Si-based solar cells have occupied most of the market for outdoor PV applications due to their mature manufacturing technologies. According to the crystalline phase, Si-based solar cells can be classified into mono-crystalline (*mc*-), poly-crystalline (*pc*-), and amorphous (*a*-) types, in which amorphous Si-based solar cells have gained considerable attention in indoor applications owing to their cost-effective manufacture from gaseous plasma sources in thin-film form. This enables them to be formed on low-cost flexible substrates and draws on the wealth of research and development spanning four decades on improving stability and lifetime. With a bandgap of 2 eV, it is suitable for IPV application and was the first technology incorporated into low-power indoor electronics (the solar/light-powered calculator perhaps being the most ubiquitous one).⁹ In the early stage, research of Si-based IPV was limited to comparing commercial solar cells under low-illumination testing environments and the lack of appropriate models.¹⁴ In 2009, Turkenburg et al. measured 41 industrial mono- and multi-crystalline Si-based cells between 0.01 and 1000 W m⁻², and they then evaluated the accuracy of modeling based on one-diode and

two-diode models.¹⁵ Later, the fill factor (FF) expression was used by the same research group to model irradiance intensity dependence on the efficiency of Si-based IPV, and reported calculations of PV power output based on spectrally resolved irradiance.¹⁶ They pointed out that hydrogenated amorphous silicon (*a*-Si:H) cells exhibited only around 8% efficiency under Standard Testing Conditions (STC), for solar cells while up to 20% under energy-efficient lighting environments. Even though *c*-Si cells showed larger efficiency under STC, only 3%–6% efficiency can be obtained under energy-efficient LED light, as shown in Table 1. The higher efficiency in *a*-Si:H is attributed to a relatively higher V_{oc} under low light associated with the relatively larger bandgap of *a*-Si:H compared to *mc*-Si. Indeed, the calculated efficiency of *a*-Si:H solar cells is around 17.68% under LED light irradiance and the real device efficiency can reach 15.2% under the irradiance of 1.1 mW cm⁻² LED light.¹⁷

In addition to incident-dependence studies on Si-based IPV, some strategies have been demonstrated to improve the photovoltaic performance of Si-based IPV. For example, a small area *mc*-Si cell was fabricated for low-flux light harvesting in the near-infrared transparency range.¹⁸ The maximum power conversion efficiency (PCE) of 17.12% and 80% external quantum efficiency (EQE) was achieved when the cell was examined under low-flux 850 nm LED illumination by inclusion a low-pressure chemical vapor deposition (LPCVD) Si₃N₄ passivation layer (Figure 2(A,B)) in the cells. Although an intensity-dependent reduction of V_{oc} suppresses the PCE under low-flux conditions, LPCVD Si₃N₄ passivation enables a shunt resistance above 10 MΩ cm⁻² (Figure 2(C,D)) and thus alleviates the degradation of PCE and EQE.

Apart from the investigation on rigid Si-based IPV, great attention has also been paid to flexible, disposable, and potentially wearable Si-based IPV for powering next-generation electronic systems.^{19–21} Figure 2(E) depicts a flexible *a*-Si:H solar cell with a Al/Ag/*a*-Si:H (n)/*a*-Si:H(i)/*a*-Si:H(p)/indium zinc oxide configuration.³ The cell provides an efficiency of 3.4% compared to a similar structure on the glass. However, there is no data on the current density-voltage (*J*-*V*) characteristics under indoor lighting conditions. Nevertheless, the cells show the potential of *a*-Si:H for low cost, large-scale production using roll-to-roll processes on flexible substrates for providing PV power in applications such as smart labels, food sensing electronics and RFID.

3.2 | DSSCs for indoor application

As one of third-generation PV devices, DSSCs are sensitive to the variation of irradiance and hence can be

TABLE 1 Silicon solar cells characteristics under STC and indoor white-LED lighting. Copyright 2009, Elsevier

	J_{sc} (μA and mA cm^{-2})			V_{oc} (V)			FF (%)			Efficiency (%)	
	LED1 μA	LED2 μA	STC mA	LED1	LED2	STC	LED1	LED2	STC	LED1/2	STC
<i>a</i> -Si:H	118	113	13.5	0.67	0.67	0.82	0.68	0.68	0.7	~19–21	7.7
<i>mc</i> -Si	138	94	~37	0.4	0.4	~0.7	0.35	0.35	~0.8	5.3–5.6	18.2
<i>pc</i> -Si	119	86	~35	0.3	0.3	~0.6	0.35	0.35	~0.8	3.6–3.7	16.8

Abbreviations: FF, fill factor; LED, light-emitting diode; STC, Standard Testing Conditions.

applied for light energy harvesting both indoors and outdoors.^{8,9} The operation of DSSCs is similar to photosynthesis which occurs inside plants, with photo-sensitization of dye on the working electrode, typically TiO_2 , generating electrons before being replenished by an electrolyte through a redox reaction.²² Since Grätzel first reported DSSCs with PCE over 7%, enormous progress has been made in both outdoor and indoor DSSCs, including synthesis of novel dyes, optimization of collecting material, and development of electrolytes.^{7,23}

Among the components in indoor DSSCs, the application of novel dyes play a significant role in effective light harvesting.⁷ Porphyrin is one type of commonly used dye sensitizer, with a high extinction coefficient, excellent stability, low synthesis cost, and efficient electron transferability.^{24,25} For example, Liu et al. synthesized a new push-pull porphyrin dye Y1A1 (structure in Figure 3(A)) for indoor DSSCs. Resultant cells showed not only superior performance with optimal PCE of 9.22% under AM1.5 G but also exhibited excellent characteristics with a V_{oc} of 0.5 V and PCE of 13.5%–19.5% under ambient lighting illumination of 300–2400 lux (Figure 3(B–D)).²⁷

Additionally, anthracene-based molecules have been used in indoor DSSCs because of their unique photo-physical properties such as bright blue electroluminescence.^{28,29} A group of metal-free anthracene-based dye molecules with donor-acceptor- π -acceptor (D-A- π -A) configuration were synthesized by Tingare et al., and they proved that sensitizer TY6 can display outstanding PCE of 20.72% and 28.56% under 6000 lux of LED and T5 fluorescent light source,²⁶ respectively, which is because of the spectral match of LED light and energy level alignment with TiO_2 for efficient electron injection.³⁰ Figure 4(A–C) are optical and electrical characteristics of anthracene-based dye TY3, TY4, and TY6 molecules in DSSCs, respectively. Other anthracene-based sensitizers were also studied, wherein AN3-based DSSCs achieved a PCE of 5.45% at 1000 lux and dye AN11-based DSSC obtained a PCE of 11.26% with a large area of 26.80 cm^2 .^{31,32}

The aforementioned improvement of indoor DSSCs not only relies on sensitizers but also other critical factors such as the selection of charge carrier blocking layers,

replacement of liquid electrolytes with solid electrolytes, and device architecture innovations. Liu et al. investigated the effect of different TiO_2 as a blocking layer on DSSCs performance. They found the sprayed compact TiO_2 enable DSSCs to obtain outstanding PCE efficiencies of 15.26% and 15.12% under low light intensities of 1001 and 250 lux, much higher than 8.56% and 6.19% in the reference cells.³³ Moreover, replacing the conventional liquid electrolyte with solid-state electrolyte facilitates the improvement in performance of indoor DSSCs. As reported recently, PCE of 15.39% and 20.63% were achieved with quasi-solid-state electrolyte under low light intensities of 200 and 600 lux, respectively.³⁴ It is worth mentioning that the optimization of device architecture is also a reliable method for obtaining better performance in indoor DSSCs. As shown in Figure 4(D–F), an advanced DSSC configuration was reported by Cao and coworkers, and a significantly high PCE of 31.8% under 1000 lux light intensity was realized using Y123/XY1b as cosensitizer.³⁵

3.3 | OSCs for indoor application

Since the first report of OSCs, significant progress has been made during the past two decades, with PCE steadily improving from less than 4% to over 15% under AM1.5 illumination.^{36–39} It was demonstrated by Freunek et al. that the optimum bandgap for harvesting indoor light is 1.9 eV instead of 1.4 eV for standard sunlight.⁴⁰ Therefore, unlike *mc*-Si cells, the donor/acceptor materials as an active layer inside OSCs usually have a better spectral match with indoor light, which can generate higher PCE in IPV applications. For example, Cutting and coworkers compared *mc*-Si, *a*-Si and copper indium gallium selenide (CIGS) with some selected OSCs.⁴¹ They found three types of OSCs (Figure 5(A)) showed remarkable PCEs under the white LED illumination, reaching 6.89%, 12.83%, and 21.04% for P3HT:PC₆₀BM: nanoparticles, P3HT: PC₆₀BM and PCE10: PC₇₀BM cells, respectively. Besides, a better indoor performing OSC was obtained by using 1',1'',4',4''-tetrahydro-di[1,4]methanonaphthaleno[5,6]fullerene-C₆₀ (ICBA) and

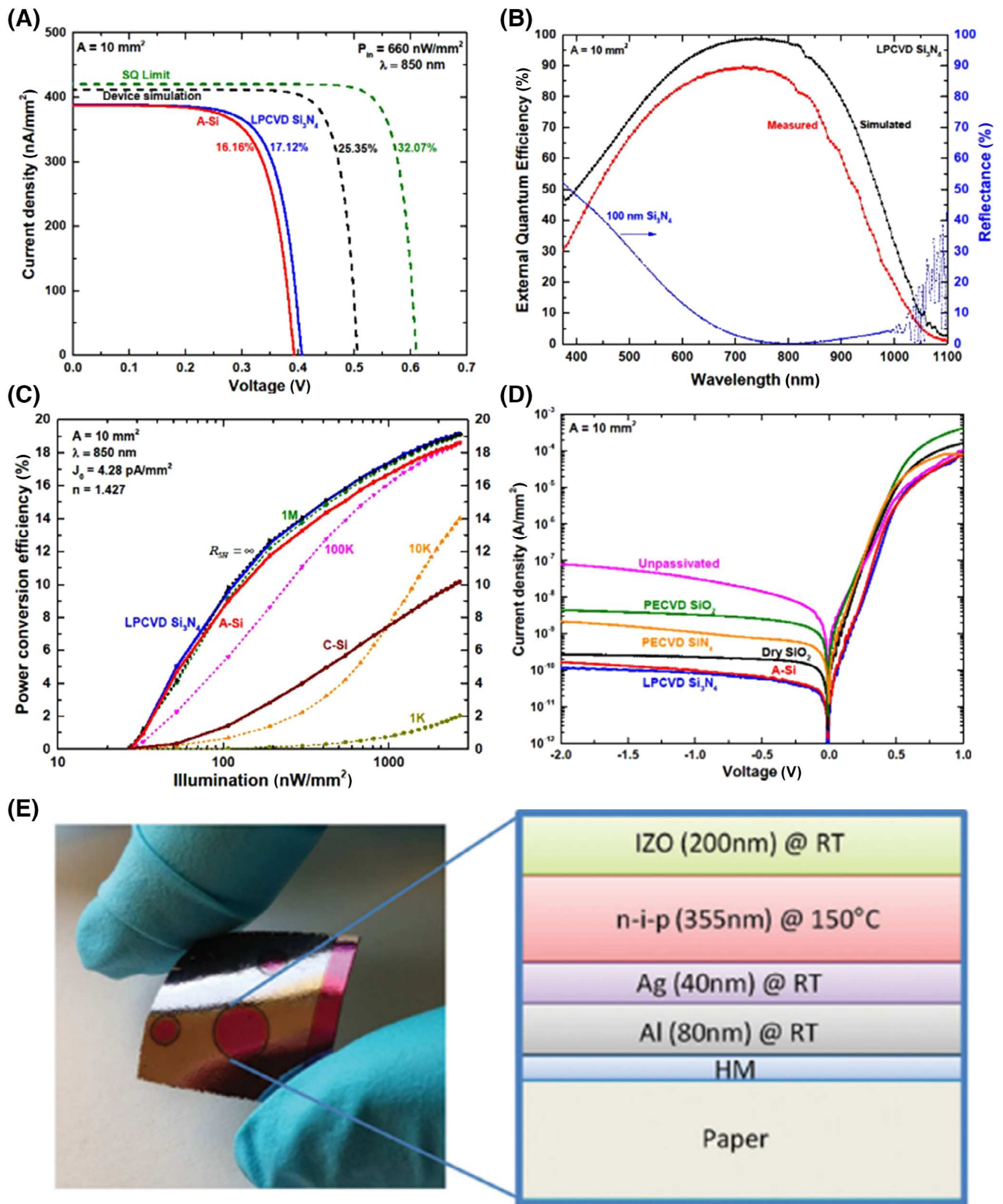


FIGURE 2 (A) J - V characteristics with the Shockley–Queisser (SQ) limit. (B) Measured and simulated external quantum efficiency (EQE) for cells with 100 nm LPCVD Si_3N_4 passivation layer. (C) Measured power conversion efficiency (PCE) dependence of near-infrared (NIR) illumination for different passivation methods. Copyright 2017, IEEE. (D) J - V under a dark condition with different passivation methods. (E) Image of a flexible a -Si:H solar cell on a paper substrate, with a schematic illustration of device configuration. Copyright 2015, Wiley-VCH

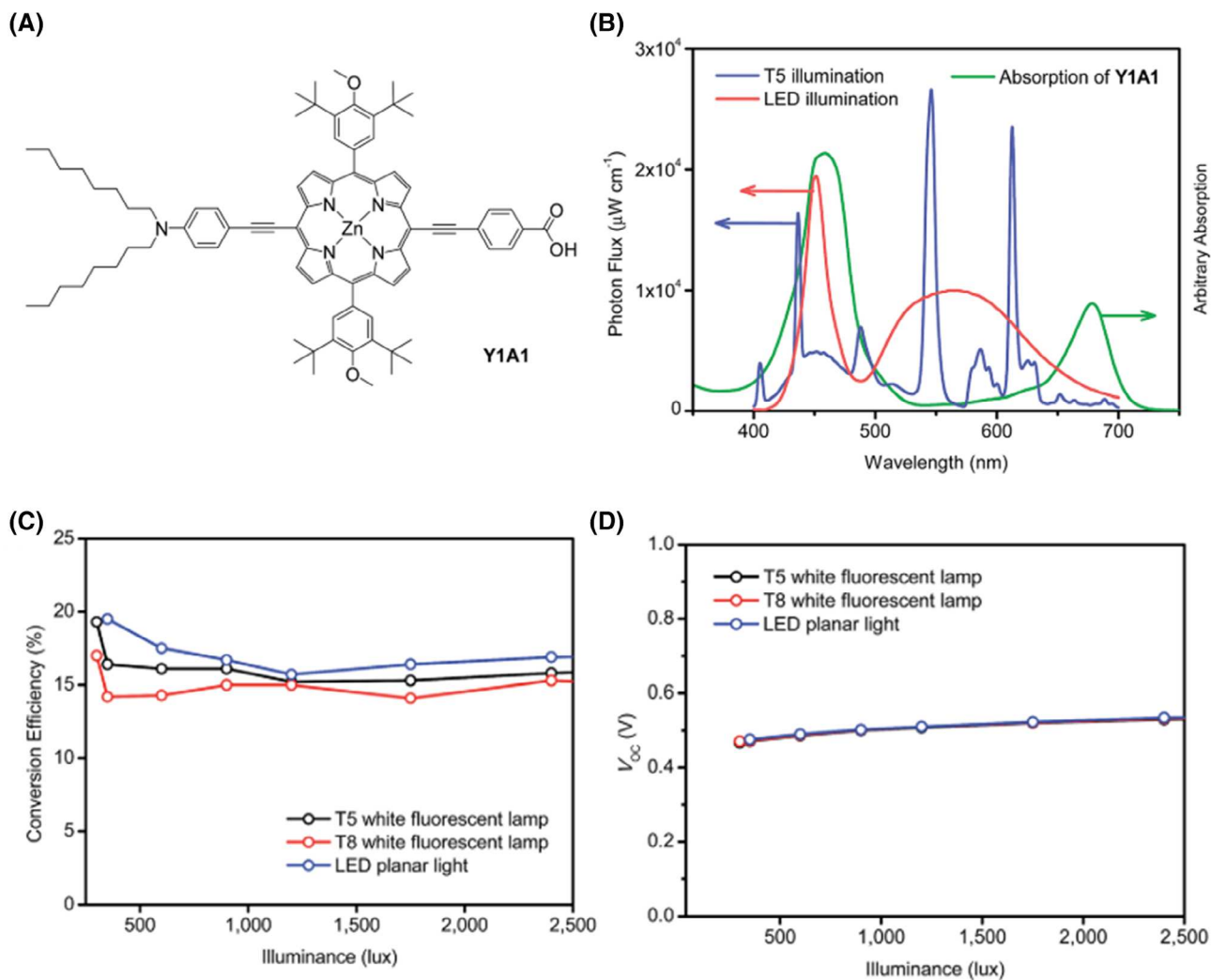


FIGURE 3 (A) Molecular structure of the porphyrin dye Y1A1. (B) Absorption spectra overlap of Y1A1 with solar irradiance, T5 illumination²⁶ and light-emitting diode (LED) illumination, respectively. (C, D) Power conversion efficiency (PCE) and V_{oc} dependence as a function of illuminance. Copyright 2016, the Royal Society of Chemistry

doping Ni into the ITO layer.⁴² The device structure and energy band diagram are shown in Figure 5(B,C). It should be pointed out that for indoor application, a high shunt resistance is crucial; however, the series resistance is not equally essential to keep a low value, in contrast to standard solar cell applications.^{9,43}

On the other hand, there is no guarantee that PCE under one sun will indicate the same characteristics under an indoor light environment, and this is closely related to the selectivity of photosensitive polymers. Lee et al. suggest that PCDTBT: PC₇₁BM OSCs outperform the PTB7: PC₇₁BM counterparts under 300 lux, generating P_{max} of $13.9 \mu\text{W cm}^{-2}$ with PCE of 16.6%, though PTB7: PC₇₁BM displayed a higher PCE under one sun, as shown in Figure 5(D–F).¹² The high performance of PCDTBT: PC₇₁BM devices under low-flux paves a way to compete with other IPVs such as *a*-Si:H IPVs that

give high efficiency under low illumination. Furthermore, a replacement of traditional fullerene-based electron-acceptor materials with nonfullerene acceptors can yield even higher indoor performance of OSCs due to greater thermal stability, photochemical stability, and longer device lifetimes induced by novel nonfullerene materials.^{44–46} In recent work by Cui et al., blending of a nonfullerene acceptor IO-4Cl and PBDB-TF polymer donor enables a 1 cm^2 OSC to obtain a PCE of 26.1%, and V_{oc} of 1.10 V under 1000 lux LED, as well as 1000 h of continuous operation under indoor light conditions.⁴⁷ As shown in Figure 6(A), light-intensity data yield a slope close to unity, which infers that the ratio of photons to electrons remains constant with decreasing light intensity. Under these three illumination conditions, PCEs ranged from 22.2% to 26.1%, attributed to high current and significantly high V_{oc} values. When it comes

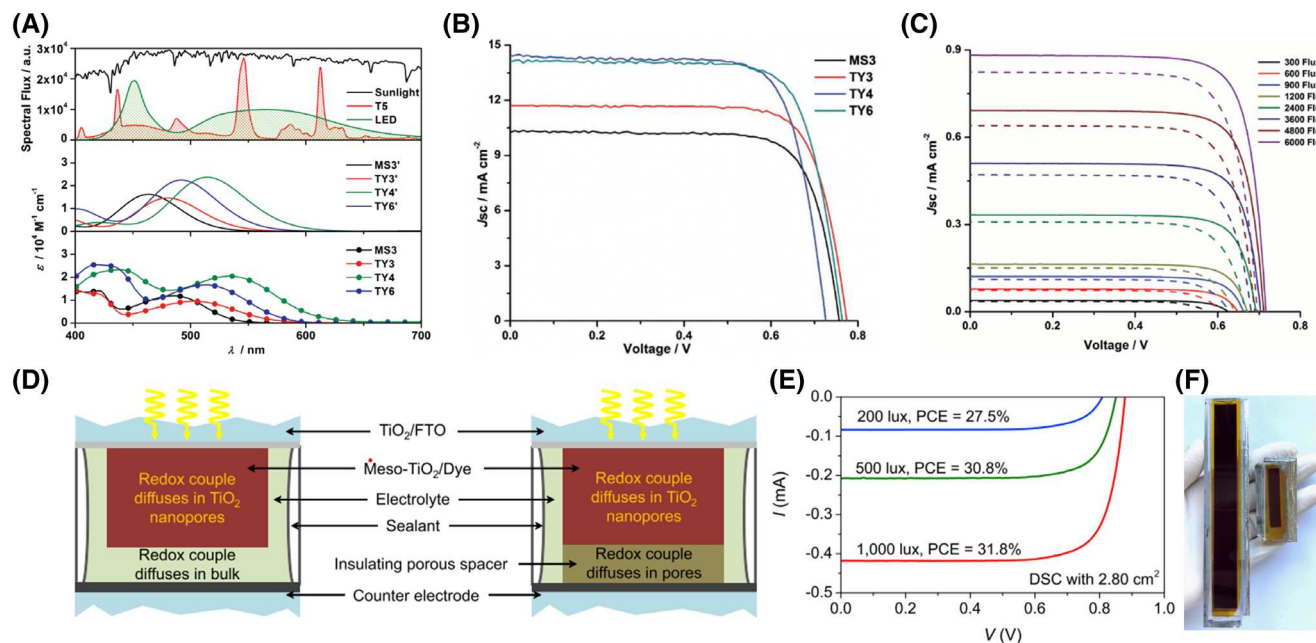


FIGURE 4 (A) The irradiance and emitting spectra of sunlight, T5, and light-emitting diode (LED) lights, with calculated and measured absorption spectra of MS3, TY3, TY4, and TY6 dyes solution. (B) J - V characteristics for DSSCs with MS3, TY3, TY4, and TY6 under AM 1.5G illumination. (C) J - V characteristics for TY6 DSSCs with (solid line) and without (dashed line) coadsorbent CDCA at different T5 light luminance. Copyright 2017, Wiley-VCH. (D) Schematic of novel DSSC architecture using p-type hole charge collector in direct contact with TiO_2 scaffold. (E) J - V curves of the DSSC of 2.80 cm^2 size under varying intensities of the indoor light. (F) Picture of two DSSCs with photoactive areas of 2.80 and 20.25 cm^2 . Copyright 2018, Elsevier

to large-area cells, a 23% PCEs under indoor illumination at 200 lux was achieved for a 4 cm^2 blade-coated cell. Interestingly, over 40% PCE is predicted through simulation (Figure 6(B,C)). This indicates a promising potential of OSCs for powering a wide range of indoor electronics. Meanwhile, a large-area module $>20 \text{ cm}^2$ with a PCE of 10.4% using a nonfullerene blend was demonstrated by Liao and coworkers, reaching PCE of 21.8% under a fluorescent lamp of 1000 lux (Figure 6(D)).⁴⁸

3.4 | Colloidal QDSCs for indoor application

Colloidal quantum dots are a type of nanoscale semiconductor crystals that exhibit unique optical, electrical properties, including size-dependent light absorption, excellent stability, high charge mobility, and facile synthesis.^{11,49–56} Till now, PCE of QDSCs has been improved up to 13%.^{13,49,57–64} However, despite many efforts being made in QDSCs, to the best of our knowledge, reports on indoor QDSCs are still lacking within the solar cell community. However, some hybrid QD-organic and QD-metal chalcogenide cells have been explored for indoor applications.

Otsuka et al. introduced Si QDs into PTB7 and PTB7-Th polymer system by mixing QDs and polymers at certain weight ratio and fabricated Si QD-based hybrid PVs generate a PCE of 3.0% and 9.7% under one sun and LED light irradiance, respectively.⁶⁵ Figure 7(A,B) depicts the energy diagram and J - V curve of the reported cells. However, it is noticeable that this PCE value is not comparable to the aforementioned Si-based PVs, DSSCs, and OSCs for indoor application, which may be resulting from undesirable charge transfer between QDs and polymers, such as high recombination rate and lack of proper QD surface functionalization.⁵⁷ In contrast, solution-processed metal chalcogenides QDSCs have shown the possibility of achieving promising IPV behavior.¹³

Very recently, Hou et al. reported colloidal metal chalcogenide-based QDSCs with a 19.5% record efficiency under 2000 lux indoor light condition and 11.6% under 1.5 Sun concentrated solar irradiance (Figure 7(C)).¹³ They also demonstrated that an extremely high exciton density could be realized by multiphoton absorption together with judicious surface ligand engineering, which lays the foundations for high-performance QDSC for IPV developments.¹³ Notably, a remarkable amount of power can be efficiently generated under various light illumination conditions, compensating for irradiance differences due to latitude and time zone variations

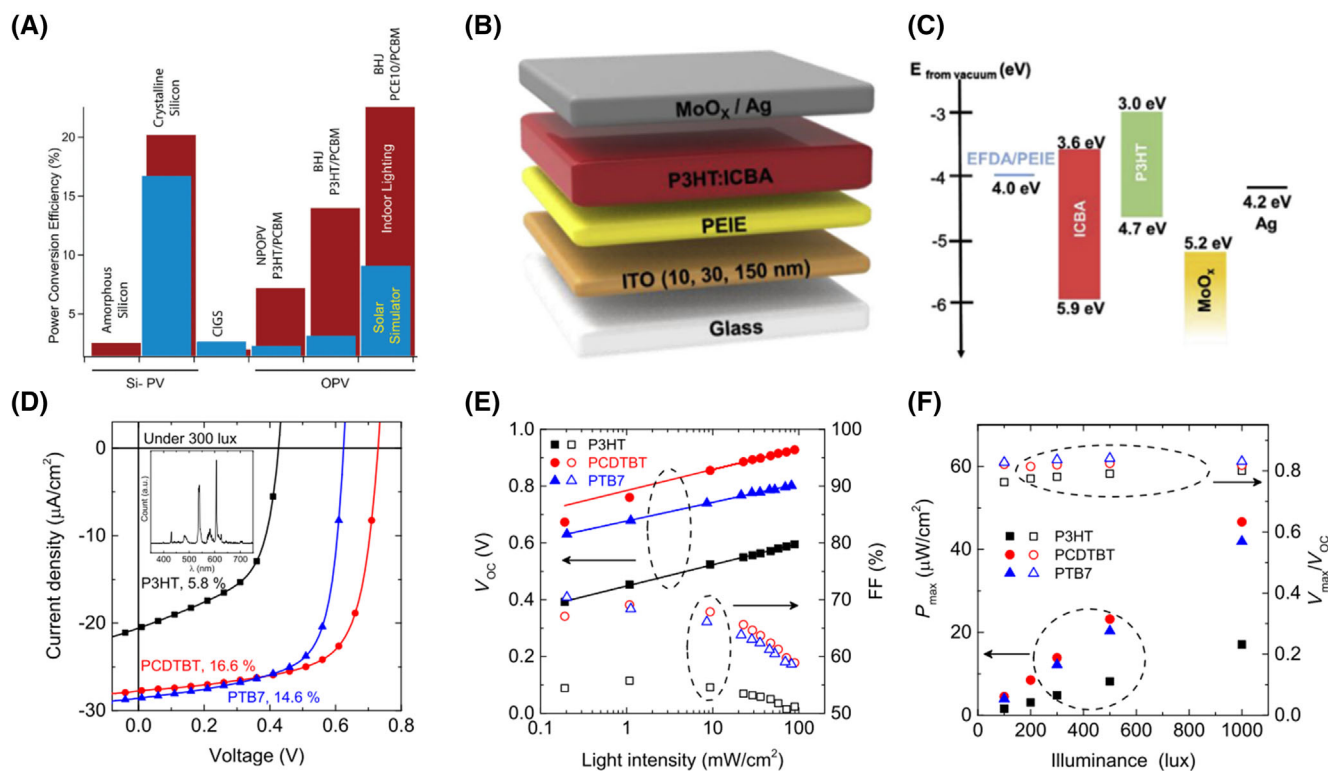


FIGURE 5 (A) Power conversion efficiency (PCE) comparison of *c*-Si, *a*-Si, CIGS, and organic solar cells (OSCs) under AM 1.5G solar simulator illumination (blue) and under light-emitting diode (LED) illumination (red). Copyright 2016, the Royal Society of Chemistry. (B) Device configuration of P3HT: ICBA inverted OSCs. (C) Energy bandgap schematics of studied OSCs. Copyright 2019, Elsevier. (D) *J*-*V* curves of P3HT:PCBM, PCDTBT:PC₇₁BM, and PTB7:PC₇₁BM devices under 300 lx fluorescent lamps. The spectrum of 300 lx fluorescent lamps is present in the inset. (E) *V*_{oc} (solid symbols) and fill factor (FF) (open symbols) of the three OSCs at a different light intensity of AM1.5 G. (F) Maximum power output density, *P*_{max} (solid symbols) and *V*_{max} to *V*_{oc} ratio (open symbols) of OSCs at different illumination levels of fluorescent lamps. Copyright 2016, the American Institute of Physics

(Figure 7(D)). Moreover, a linear increase in the short-circuit current (*J*_{sc}) and a semi-logarithmic increase in the *V*_{oc} with increasing light intensity from 0.01 to 1000 mW cm⁻² can be observed, as shown in Figure 7(E).

3.5 | PSCs for indoor application

Beyond the IPV systems described above, metal halide PSCs have also emerged as a promising alternative for indoor application.⁶⁶⁻⁷⁰ Chen et al. conducted the first investigation on indoor PSC in 2015, wherein they precisely controlled traps in the perovskite active layer and carrier dynamics via designing electron transfer layer (ETL) and thus successively made a PSC with 27.4% PCE under indoor environment.⁷¹ Notably, as presented in Figure 8(A), there is only negligible hysteresis behavior in the *J*-*V* curves, indicating an incident-light-dependent hysteresis characteristic that is more likely to occur under one sun but not low light intensity conditions. Besides, a large-area device of 5.44 cm² also exhibited a high PCE of 20.4% and promising long-term stability. Optimization of the ETL was shown to be an effective method to further improve PSC performance under indoor light.

A mesoporous TiO₂ layer was incorporated into PSCs by atomic layer deposition (ALD), spray pyrolysis (SP), and the sol-gel (SG) by Di Giacomo et al.⁷² Among these, PSCs with ALD TiO₂ layer was found to be superior in terms of *J*_{sc}, *V*_{oc}, dark current, FF and PCE, with PCE reaching 24% under 200 lux compared to 14.3% and 9.3% for the other two equivalents. The cross-sectional scanning electron microscopy in Figure 8(B) illustrates a clear planar structure inside the best PSCs. Also, Dagar et al. reported a CH₃NH₃PbI₃-based planar PSC incorporating solution-processed SnO₂/MgO composite ETL, which achieved a 25% PCE under 200 lux indoor illumination.⁷³ It was seen that the MgO layer plays an essential role since MgO can largely suppress hysteresis under both 200 and 400 lux illumination (Figure 8(C,D)). Perovskite compound is generally represented as ABC₃ where A site can be Methylammonium (MA), formamidinium (FA), cesium (Cs) single cations, or MA-FA-Cs triple cations and where B site can be occupied by Pb and C are usually halide or mixture of halide ions.^{74,75} The adjusting stoichiometric ratio of halide ions or using triple cations may bring about the possibility of better PSC performance as a result of a closer bandgap to 1.9 eV. Accordingly, Br⁻ ions were added into the PSCs to increase their bandgap values by Wu et al.

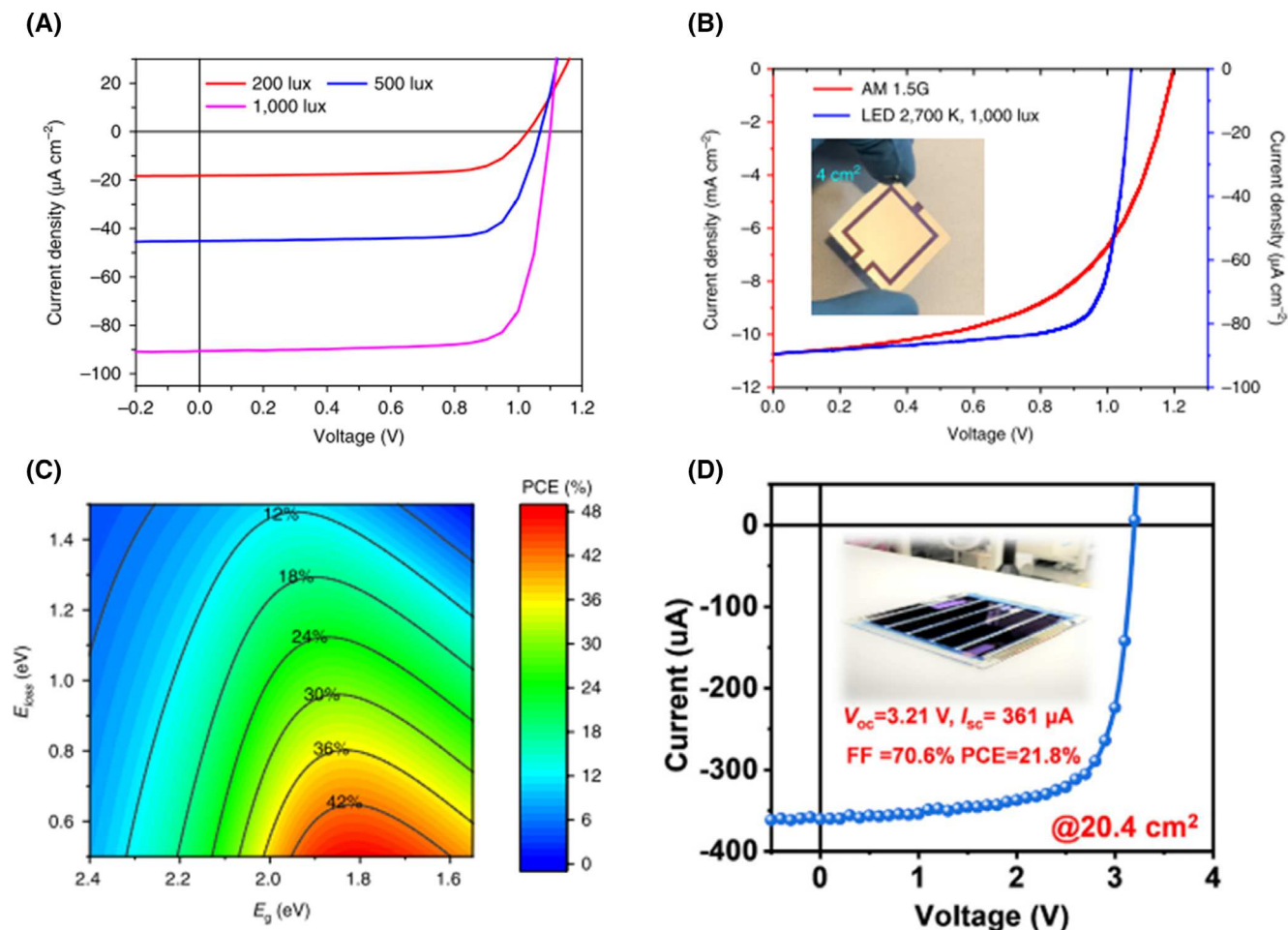


FIGURE 6 (A) *J*-*V* curves of the PBDB-TF: IO-4Cl-based cell under different indoor light intensities. (B) *J*-*V* curves of a 4 cm² organic solar cells (OSCs) via blade-coating method under AM 1.5 and light-emitting diode (LED) lighting. (C) Efficiency prediction of OSCs under LED lighting condition, with color scale bar indicating power conversion efficiencies (PCEs) of corresponding colors. Copyright 2019, Springer Nature. (D) *J*-*V* characteristics of TPD-3F-51K: IT-4F module under a fluorescent lamp with a luminance of 1000 lux. Insert is a photo of the OSC module. Copyright 2019, Elsevier

They demonstrated the bandgap of $\text{MA}_{0.85}\text{Cs}_{0.15}\text{Pb}(\text{I}_{0.85}\text{Br}_{0.15})_3$ can be enlarged to 1.66 eV, which resulted in the highest PCEs of 25.94% and 25.12% under illumination from fluorescent tubes and a white LED.⁷⁶ Similarly, Cheng et al. reported a triple-anion $\text{CH}_3\text{NH}_3\text{PbI}_{2-x}\text{BrCl}_x$ PSCs with a specially tailored bandgap. As shown in Figure 8(E,F), a record high efficiency of 36.2% was achieved with a distinctive high V_{oc} of 1.028 V.⁷⁷ Meanwhile, their large-area cells obtained a PCE of 30.6% and long-term stability, sustaining >95% of the original efficiency under continuous light soaking over 2000 h.

4 | CHALLENGES AND PROSPECTS

In summary, the basic concept and design principles of IPV are introduced. We also provide a summary of the

development of Si-based PVs, DSSCs, OSCs, QDSCs, and PSCs under indoor light conditions. Despite exciting progress during past decades, it is still challenging to design high efficiency indoor solar cells and maintain their long-term performance under identical operating conditions. Thus, further improvement is required before commercialization occurs. In particular, IPV optimization is strongly dependent on cell material composition and device designs.

For Si IPVs, intrinsic spectra mismatch and variable performances due to device structure design are still the barriers to better IPV performance. As calculated by Bahrami-Yekta, the optimum thickness of *a*-Si solar cell for indoor applications is supposed to be 1.8 μm .⁷⁸ So unlike high absorption coefficient QD and perovskite thin films (few hundred-nanometer thicknesses, for instance), Si cannot yield equivalent efficiency with the same film thickness, which means material purity may become a concern. This results in an inevitable trade-off

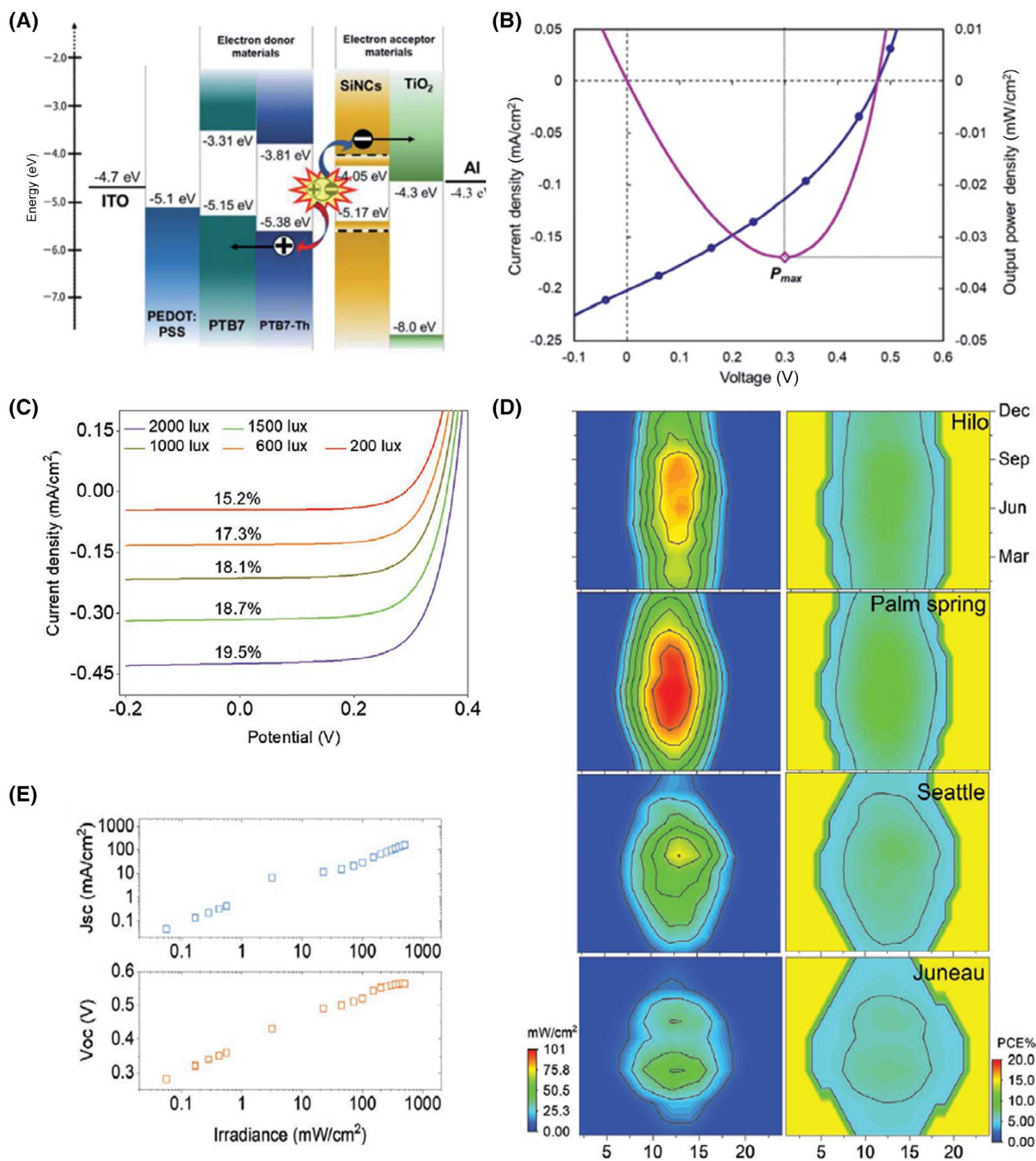


FIGURE 7 (A) Energy diagram of quantum dot (QD)-polymer hybrid PV device. Copyright 2020, The Royal Society of Chemistry. (B) *J-V* characteristics of Si-based QD-polymer hybrid PV device under 1000 lx indoor light. (C) *J-V* curves and power conversion efficiency (PCE) values of QD solar cells (QDSCs) under different indoor light illumination. (D) Left panel shows mean annual daily irradiance of four US cities among different LA and right panel shows simulated mean annual daily QDSC efficiency from selected cities. (E) *J*_{sc} and *V*_{oc} dependence on irradiance. Copyright 2020, Wiley-VCH

between device performance and material consumption during the complex device fabrication process.

Compared to Si-based IPVs, DSSCs tend to be more cost-effective and processable. However, the use of costly

ruthenium-based dye, the platinum-catalyzed counter electrode, and transparent electrodes remains as concerns for indoor DSSCs.^{9,79,80} Liquid electrolytes inside DSSCs can also suffer from the risk of safety and potential

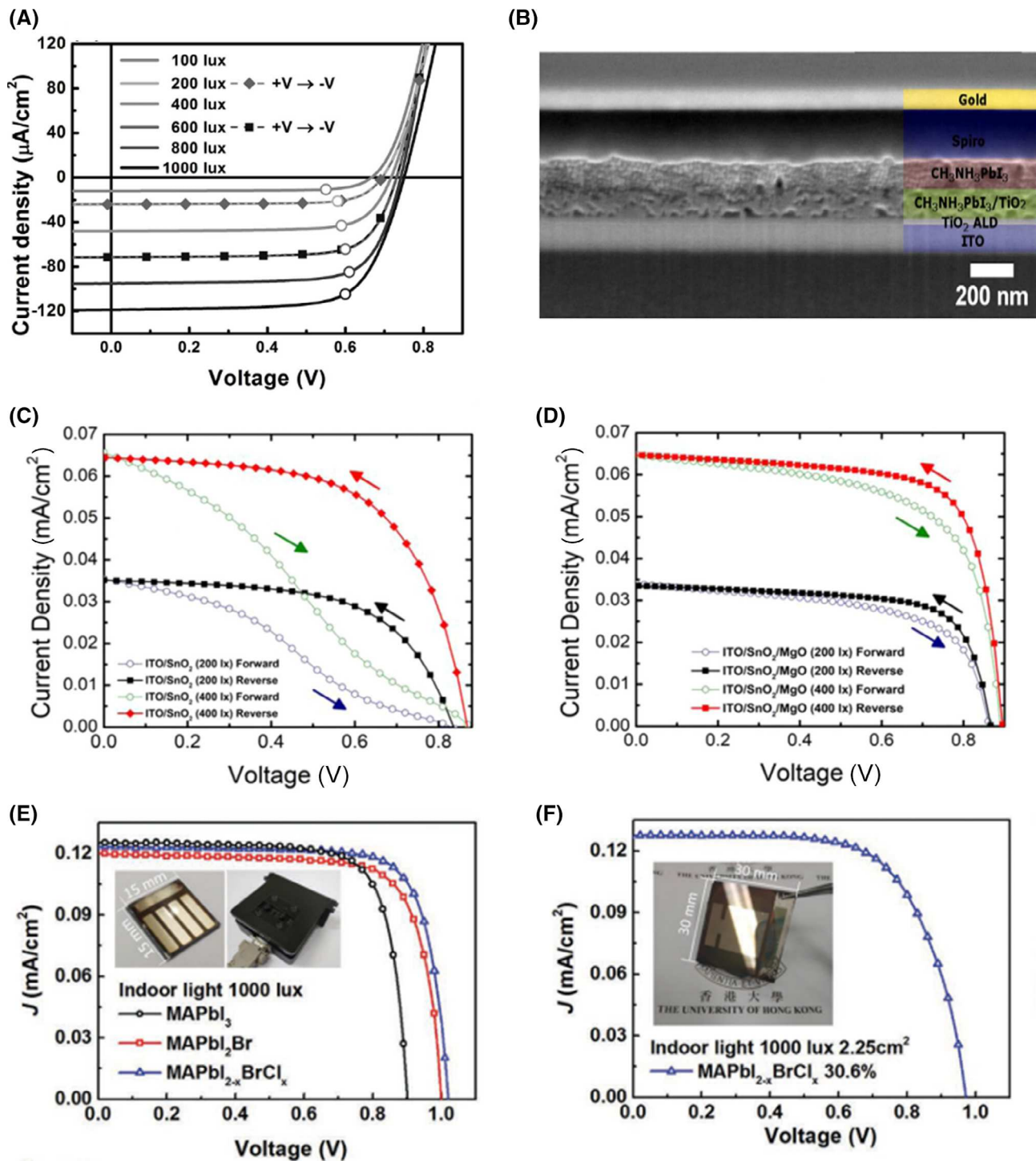


FIGURE 8 (A) J - V characteristics of perovskite solar cells (PSCs) with two-step PCBM as an electron transfer layer. The solid lines and dashed lines represent the sweeping direction from negative to positive bias and from positive to negative bias, respectively. Copyright 2015, Wiley-VCH. (B) Cross-sectional SEM image of a Glass/ITO/TiO₂ ALD/TiO₂ mesoUV/ CH₃NH₃PbI₃/Spiro-OMeTAD/Au PSC. Copyright 2016, Elsevier. (C) J - V curves of ITO/SnO₂ based PSCs under 200 and 400 lx in both forward and reverse bias scanning directions. Copyright 2018, Elsevier. (D) J - V curves of ITO/SnO₂/MgO composite based PSCs under 200 and 400 lx in both forward and reverse bias scanning directions. Copyright 2018, Elsevier. (E) J - V curves of the three groups of devices under 1000 lux indoor light (2700 K fluorescent). Inset shows the PSCs (1.5 × 1.5 cm²) and the test holder for 0.1 cm² active area. (F) J - V curve of the large area device (3 × 3 cm² with an active area of 1.5 × 1.5 cm²) under 1000 lux indoor light (2700 K fluorescent). Copyright 2019, Wiley-VCH

leakage and degradation. As previously discussed, replacing the liquid electrolyte with a solid-state counterpart is a promising solution to this problem. For instance, in a quasi-solid-state DSSCs, 97% of the initial PCEs can remain after 1000 h test under 200 lux light illumination in an ambient atmosphere.³⁴

The limitation for OSCs under indoor illumination lies in the active layer degradation due to sensitivity of moisture, oxygen, and UV light as well as parasitic resistance, which relies on different illumination conditions.^{81,82} Also, since fullerene is commonly used as acceptor material in OSCs, thermally induced aggregates and its intrinsic physical energy loss may adversely affect the morphology of active layer, limit V_{oc} and hence performance of OSCs.^{83,84} For example, recent research has shown that PCBM increases sensitivity of OSCs to oxygen and moisture since PCBM will undergo modification upon prolonged oxygen or water exposure, which will severely degrade transport properties inside the PCBM domains and thus impact on the performance of OSCs.⁸⁵ Therefore, nonfullerene OSC systems would be a desirable alternative. However, a more in-depth understanding of degradation mechanisms, especially under different low-flux irradiance conditions, is still needed.

To date, there are only a few reports on QDSCs performance in indoor environments, which may be due to relatively lower PCE of QDSCs under standard AM 1.5G outdoor conditions. However, QDs themselves are promising nanoscale zero-dimensional materials which have tunable bandgaps, the discrete density of states, high absorption coefficient, and large-scale processibility. We believe, after the recent seminal work demonstrated by Hou et al.,¹³ more exciting results will come in the near future.

PSCs are one of the most promising candidates for IPV application due to their high absorption coefficient, high charge mobility, facile synthesis, and distinctly high defect tolerance. Although Pb-based PSCs have exhibited excellent performance in indoor application, they also feature some shortcomings that should be addressed to enable their long-term stable use. Generally, these limitations are related to the toxicity of heavy metals, high sensitivity to oxygen and water, as well as unsuitable electronic band structure.⁹ Toxicity is one of the most significant limitations in PSCs, mainly due to Pb, which is harmful to humans and environment, and this raises the importance of fundamentally addressing the toxicity issues through chemical composition engineering.^{86,87} Tin-based perovskites could be able to address toxicity problem, and self-healing encapsulation materials and the incorporation of neutralizers and precipitants such as sulfides may be an effective strategy.⁸⁷ Another issue of concern involves instability of perovskite thin films and heightens toxicity concerns as perovskite compounds are unstable due to their sensitivity to moisture, oxygen, heat may result in toxic Pb leakage.^{88,89} Since the stability of

halide perovskite compounds is mutually related to their toxicity, similar measures mentioned above, such as compositional engineering and advanced encapsulation needs to be explored.⁸⁹ Moreover, typical perovskite compounds MAPbI₃ exhibit relatively narrow electronic bandgaps around 1.6 eV, which are less favorable for indoor light harvesting. To enlarge the bandgap of halide perovskite approaches such as lattice expansion by incorporating halide double perovskites may be required.

Apart from the abovementioned challenges in each type of IPV, the metrology of IPVs under various indoor radiations has not yet been standardized. Illumination conditions are not uniform as those in the standard AM 1.5G testing condition, including the type of lighting source, intensity, and wavelength. So, the standardization of indoor testing protocols is necessarily required. Under the ambient low light conditions, the device operation mechanisms of indoor thin-film PVs will change. However, to date, research on IPV cell modeling and operation mechanisms are still lacking. Also, there are few studies on long-term stability characterizations under indoor conditions. Nevertheless, considering how much progress has been made in solution-processed solar cells and how many challenges needed to be overcome, there is no doubt that the realization of IPV devices will be *the next big trend* in solution-processed Photovoltaics.

ACKNOWLEDGMENTS

G. A. J. Amaratunga gratefully acknowledge the funding from the Engineering and Physical Sciences Research Council (EPSRC, EP/P027628/1). B. Hou acknowledges the financial support by the Cardiff University.

CONFLICT OF INTEREST

The authors declared no potential conflicts of interest.

ORCID

Gehan A. J. Amaratunga  <https://orcid.org/0000-0002-8614-2864>

REFERENCES

1. Nelson J. *The Physics of Solar Cells*. London: Imperial College Press; 2003.
2. Petter Jelle B, Breivik C, Drolsum Røkenes H. Building integrated photovoltaic products: a state-of-the-art review and future research opportunities. *Sol Energy Mater Sol Cells*. 2012; 100:69-96.
3. Águas H, Mateus T, Vicente A, et al. Thin film silicon photovoltaic cells on paper for flexible indoor applications. *Adv Funct Mater*. 2015;25(23):3592-3598.
4. Lee TD, Ebong AU. A review of thin film solar cell technologies and challenges. *Renew Sustain Energy Rev*. 2017;70:1286-1297.

5. Mathews I, Kantareddy SN, Buonassisi T, Peters IM. Technology and market perspective for indoor photovoltaic cells. *Joule*. 2019;3(6):1415-1426.
6. Mainville M, Leclerc M. Recent progress on indoor organic photovoltaics: from molecular design to production scale. *ACS Energy Lett*. 2020;5(4):1186-1197.
7. Freitag M, Teuscher J, Saygili Y, et al. Dye-sensitized solar cells for efficient power generation under ambient lighting. *Nat Photonics*. 2017;11(6):372-378.
8. Yan N, Zhao C, You S, Zhang Y, Li W. Recent progress of thin-film photovoltaics for indoor application. *Chin Chem Lett*. 2020;31(3):643-653.
9. Li M, Igbari F, Wang ZK, Liao LS. Indoor thin-film photovoltaics: progress and challenges. *Adv Energy Mater*. 2020;10(28):2000641.
10. Apostolou G, Verwaal M, Reinders A. Estimating the performance of product integrated photovoltaic (PIPV) cells under indoor conditions for the support of design processes. *Proceedings of the 40th IEEE Photovoltaics Specialists Conference (PVSC); IEEE*. 2014;742-747.
11. Li B, Lu M, Feng J, et al. Colloidal quantum dot hybrids: an emerging class of materials for ambient lighting. *J Mater Chem C*. 2020;8(31):10676-10695.
12. Lee HK, Li Z, Durrant JR, Tsoi WC. Is organic photovoltaics promising for indoor applications? *Appl Phys Lett*. 2016;108(25):253301.
13. Hou B, Kim BS, HKH L, et al. Multiphoton absorption stimulated metal chalcogenide quantum dot solar cells under ambient and concentrated irradiance. *Adv Funct Mater*. 2020;30(39):2004563.
14. Randall JF, Jacot J. Is AM1.5 applicable in practice? Modelling eight photovoltaic materials with respect to light intensity and two spectra. *Renew Energy*. 2003;28(12):1851-1864.
15. Reich NH, van Sark WJHM, Alsema EA, et al. Crystalline silicon cell performance at low light intensities. *Sol Energy Mater Sol Cells*. 2009;93(9):1471-1481.
16. Reich NH, van Sark WJHM, Turkenburg WC. Charge yield potential of indoor-operated solar cells incorporated into product integrated photovoltaic (PIPV). *Renew Energy*. 2011;36(2):642-647.
17. Yang P, Chan I, Lin C, Chang Y. Thin film solar cells for indoor use. *Proceedings of the 37th IEEE Photovoltaics Specialists Conference (PVSC); IEEE*. 2011;696-698.
18. Moon E, Blaauw D, Phillips JD. Small-area Si Photovoltaics for low-flux infrared energy harvesting. *IEEE Trans Electron Devices*. 2017;64(1):15-20.
19. Martins R, Ferreira I, Fortunato E. Electronics with and on paper. *Phys Status Solidi RRL*. 2011;5(9):332-335.
20. Haug FJ, Söderström T, Python M, Terrazzoni-Daudrix V, Niquille X, Ballif C. Development of micromorph tandem solar cells on flexible low-cost plastic substrates. *Sol Energy Mater Sol Cells*. 2009;93(6):884-887.
21. Schubert MB, Werner JH. Flexible solar cells for clothing. *Mater Today*. 2006;9(6):42-50.
22. Bella F, Gerbaldi C, Barolo C, Grätzel M. Aqueous dye-sensitized solar cells. *Chem Soc Rev*. 2015;44(11):3431-3473.
23. O'Regan B, Grätzel M. A low-cost, high-efficiency solar cell based on dye-sensitized colloidal TiO₂ films. *Nature*. 1991;353(6346):737-740.
24. Shalini S, Balasundaraprabhu R, Kumar TS, Prabavathy N, Senthilarasu S, Prasanna S. Status and outlook of sensitizers/dyes used in dye sensitized solar cells (DSSC): a review. *Int J Energy Res*. 2016;40(10):1303-1320.
25. Higashino T, Imahori H. Porphyrins as excellent dyes for dye-sensitized solar cells: recent developments and insights. *Dalton Trans*. 2015;44(2):448-463.
26. Chen T-A, Wu X, Rieke RD. Regiocontrolled synthesis of poly (3-alkylthiophenes) mediated by Rieke zinc: their characterization and solid-state properties. *J Am Chem Soc*. 1995;117(1):233-244.
27. Liu Y-C, Chou H-H, Ho F-Y, Wei H-J, Wei T-C, Yeh C-Y. A feasible scalable porphyrin dye for dye-sensitized solar cells under one sun and dim light environments. *J Mater Chem A*. 2016;4(30):11878-11887.
28. Srinivas K, Yesudas K, Bhanuprakash K, Rao VJ, Giribabu L. A combined experimental and computational investigation of anthracene based sensitizers for DSSC: comparison of cyanoacrylic and malonic acid electron withdrawing groups binding onto the TiO₂ anatase (101) surface. *J Phys Chem C*. 2009;113(46):20117-20126.
29. Cha H, Chung DS, Bae SY, et al. Complementary absorbing star-shaped small molecules for the preparation of ternary cascade energy structures in organic photovoltaic cells. *Adv Funct Mater*. 2013;23(12):1556-1565.
30. Tingare YS, NSN V, Chou H-H, et al. New acetylene-bridged 9,10-conjugated anthracene sensitizers: application in outdoor and indoor dye-sensitized solar cells. *Adv Energy Mater*. 2017;7(18):1700032.
31. Wang C-L, Lin P-T, Wang Y-F, et al. Cost-effective anthryl dyes for dye-sensitized cells under one sun and dim light. *J Phys Chem C*. 2015;119(43):24282-24289.
32. Tsai M-C, Wang C-L, Chang C-W, et al. A large, ultra-black, efficient and cost-effective dye-sensitized solar module approaching 12% overall efficiency under 1000 lux indoor light. *J Mater Chem A*. 2018;6(5):1995-2003.
33. Liu IP, Lin W-H, Tseng-Shan C-M, Lee Y-L. Importance of compact blocking layers to the performance of dye-sensitized solar cells under ambient light conditions. *ACS Appl Mater Interfaces*. 2018;10(45):38900-38905.
34. Venkatesan S, Liu IP, Hung W-N, Teng H, Lee Y-L. Highly efficient quasi-solid-state dye-sensitized solar cells prepared by printable electrolytes for room light applications. *Chem Eng J*. 2019;367:17-24.
35. Cao Y, Liu Y, Zakeeruddin SM, Hagfeldt A, Grätzel M. Direct contact of selective charge extraction layers enables high-efficiency molecular photovoltaics. *Joule*. 2018;2(6):1108-1117.
36. Yuan J, Zhang Y, Zhou L, et al. Single-junction organic solar cell with over 15% efficiency using fused-ring acceptor with electron-deficient core. *Joule*. 2019;3(4):1140-1151.
37. Niotaki K, Collado A, Georgiadis A, Kim S, Tentzeris MM. Solar/electromagnetic energy harvesting and wireless power transmission. *Proc IEEE*. 2014;102(11):1712-1722.
38. Abeygunasekara WL, Hiralal P, Samaranayake L, et al. Incorporating semiconducting single-walled carbon nanotubes as efficient charge extractors in organic solar cells. *Appl Phys Lett*. 2015;106(12):123305.
39. Abeygunasekara W, Samaranayake L, Karunaratne V, Amaratunga G. Generation profile shape dependent performance of mobility imbalanced organic solar cells. *Proceedings of the 10th IEEE International Conference on Industrial and Information Systems (CIIS); IEEE*. 2015;354-359.
40. Freunek M, Freunek M, Reindl LM. Maximum efficiencies of indoor photovoltaic devices. *IEEE J Photovolt*. 2013;3(1):59-64.
41. Cutting CL, Bag M, Venkataraman D. Indoor light recycling: a new home for organic photovoltaics. *J Mater Chem C*. 2016;4(43):10367-10370.
42. Kim YW, Goo JS, Lee TH, et al. Tailoring Opto-electrical properties of ultra-thin indium tin oxide films via filament doping:

- application as a transparent cathode for indoor organic photovoltaics. *J Power Sources*. 2019;424:165-175.
43. Park SY, Li Y, Kim J, et al. Alkoxybenzothiadiazole-based fullerene and nonfullerene polymer solar cells with high shunt resistance for indoor photovoltaic applications. *ACS Appl Mater Interfaces*. 2018;10(4):3885-3894.
 44. Hou J, Inganäs O, Friend RH, Gao F. Organic solar cells based on non-fullerene acceptors. *Nat Mater*. 2018;17(2):119-128.
 45. Yan C, Barlow S, Wang Z, et al. Non-fullerene acceptors for organic solar cells. *Nat Rev Mater*. 2018;3(3):18003.
 46. Zhang G, Zhao J, Chow PCY, et al. Nonfullerene acceptor molecules for bulk heterojunction organic solar cells. *Chem Rev*. 2018;118(7):3447-3507.
 47. Cui Y, Wang Y, Bergqvist J, et al. Wide-gap non-fullerene acceptor enabling high-performance organic photovoltaic cells for indoor applications. *Nat Energy*. 2019;4(9):768-775.
 48. Liao C-Y, Chen Y, Lee C-C, et al. Processing strategies for an organic photovoltaic module with over 10% efficiency. *Joule*. 2020;4(1):189-206.
 49. Hou B. Colloidal quantum dots: the artificial building blocks for new-generation photo-electronics and. *Photochemistry*. 2019;59(8):637-638.
 50. Hou B, Li Y, Liu Y, Yuan B, Jia M, Jiang F. A simple way of shape-controlled synthesis of ZnSe nanocrystals: nanodots, nanoflowers, and nanotubes. *CrystEngComm*. 2009;11(9):1789-1792.
 51. Hou B, Liu Y, Li Y, Yuan B, Jia M, Jiang F. Evolution of soft templates in surfactant/cosurfactant system for shape control of ZnSe nanocrystals. *Mater Sci Eng B*. 2012;177(5):411-415.
 52. Hou B, Parker D, Kissling GP, Jones JA, Cherns D, Fermín DJ. Structure and band edge energy of highly luminescent CdSe_{1-x}Te_x alloyed quantum dots. *J Phys Chem C*. 2013;117(13):6814-6820.
 53. Hou B, Benito-Alifonso D, Webster R, Cherns D, Galan MC, Fermín DJ. Rapid phosphine-free synthesis of CdSe quantum dots: promoting the generation of Se precursors using a radical initiator. *J Mater Chem A*. 2014;2(19):6879-6886.
 54. Benito-Alifonso D, Tremel S, Hou B, et al. Lactose as a "Trojan horse" for quantum dot cell transport. *Angew Chem Int Ed*. 2014;53(3):810-814.
 55. Hou B, Jung S-H, Zhang J, et al. Growth of quantum dot coated core-shell anisotropic nanowires for improved thermal and electronic transport. *Appl Phys Lett*. 2019;114(24):243104.
 56. Hou B, Sohn M, Lee Y-W, et al. Chemically encoded self-organized quantum chain supracrystals with exceptional charge and ion transport properties. *Nano Energy*. 2019;62:764-771.
 57. Li B, Kim JM, Amaratunga GA. Inorganic quantum dot materials and their applications in "organic" hybrid solar cells. *Isr J Chem*. 2019;59(8):720-728.
 58. Choi M-J, de Arquer FPG, Proppe AH, et al. Cascade surface modification of colloidal quantum dot inks enables efficient bulk homojunction photovoltaics. *Nat Commun*. 2020;11(1):1-9.
 59. Liu M, Voznyy O, Sabatini R, et al. Hybrid organic-inorganic inks flatten the energy landscape in colloidal quantum dot solids. *Nat Mater*. 2017;16(2):258-263.
 60. Kim B-S, Hong J, Hou B, et al. Inorganic-ligand exchanging time effect in PbS quantum dot solar cell. *Appl Phys Lett*. 2016;109(6):063901.
 61. Hou B, Cho Y, Kim BS, et al. Highly monodispersed PbS quantum dots for outstanding cascaded-junction solar cells. *ACS Energy Lett*. 2016;1(4):834-839.
 62. Baek S-W, Jun S, Kim B, et al. Efficient hybrid colloidal quantum dot/organic solar cells mediated by near-infrared sensitizing small molecules. *Nat Energy*. 2019;4(11):969-976.
 63. Sun B, Johnston A, Xu C, et al. Monolayer perovskite bridges enable strong quantum dot coupling for efficient solar cells. *Joule*. 2020;4(7):1542-1556.
 64. Chuang CM, Brown PR, Bulović V, Bawendi MG. Improved performance and stability in quantum dot solar cells through band alignment engineering. *Nat Mater*. 2014;13(8):796-801.
 65. Otsuka M, Kurokawa Y, Ding Y, et al. Silicon nanocrystal hybrid photovoltaic devices for indoor light energy harvesting. *RSC Adv*. 2020;10(21):12611-12618.
 66. Liu M, Johnston MB, Snaith HJ. Efficient planar heterojunction perovskite solar cells by vapour deposition. *Nature*. 2013;501(7467):395-398.
 67. Correa-Baena J-P, Saliba M, Buonassisi T, et al. Promises and challenges of perovskite solar cells. *Science*. 2017;358(6364):739-744.
 68. Park N-G, Zhu K. Scalable fabrication and coating methods for perovskite solar cells and solar modules. *Nat Rev Mater*. 2020;5(5):333-350.
 69. Di Giacomo F, Fakharuddin A, Jose R, Brown TM. Progress, challenges and perspectives in flexible perovskite solar cells. *Energ Environ Sci*. 2016;9(10):3007-3035.
 70. Ann MH, Kim J, Kim M, et al. Device design rules and operation principles of high-power perovskite solar cells for indoor applications. *Nano Energy*. 2020;68:104321.
 71. Chen C-Y, Chang J-H, Chiang K-M, Lin H-L, Hsiao S-Y, Lin H-W. Perovskite photovoltaics for dim-light applications. *Adv Funct Mater*. 2015;25(45):7064-7070.
 72. Di Giacomo F, Zardetto V, Lucarelli G, et al. Mesoporous perovskite solar cells and the role of nanoscale compact layers for remarkable all-round high efficiency under both indoor and outdoor illumination. *Nano Energy*. 2016;30:460-469.
 73. Dagar J, Castro-Hermosa S, Lucarelli G, Cacialli F, Brown TM. Highly efficient perovskite solar cells for light harvesting under indoor illumination via solution processed SnO₂/MgO composite electron transport layers. *Nano Energy*. 2018;49:290-299.
 74. Lee MM, Teuscher J, Miyasaka T, Murakami TN, Snaith HJ. Efficient hybrid solar cells based on meso-superstructured organometal halide perovskites. *Science*. 2012;338(6107):643-647.
 75. Saliba M, Matsui T, Seo J-Y, et al. Cesium-containing triple cation perovskite solar cells: improved stability, reproducibility and high efficiency. *Energ Environ Sci*. 2016;9(6):1989-1997.
 76. Wu M-J, Kuo C-C, Jhuang L-S, Chen P-H, Lai Y-F, Chen F-C. Bandgap engineering enhances the performance of mixed-cation perovskite materials for indoor photovoltaic applications. *Adv Energy Mater*. 2019;9(37):1901863.
 77. Cheng R, Chung C-C, Zhang H, et al. Tailoring triple-anion perovskite material for indoor light harvesting with restrained halide segregation and record high efficiency beyond 36%. *Adv Energy Mater*. 2019;9(38):1901980.
 78. Bahrami-Yekta V, Tiedje T. Limiting efficiency of indoor silicon photovoltaic devices. *Opt Express*. 2018;26(22):28238-28248.
 79. Lee C-P, Lin C-A, Wei T-C, et al. Economical low-light photovoltaics by using the Pt-free dye-sensitized solar cell with graphene dot/PEDOT:PSS counter electrodes. *Nano Energy*. 2015;18:109-117.
 80. Lee C-P, Lai K-Y, Lin C-A, et al. A paper-based electrode using a graphene dot/PEDOT: PSS composite for flexible solar cells. *Nano Energy*. 2017;36:260-267.

81. Shin S-C, Koh CW, Vincent P, et al. Ultra-thick semi-crystalline photoactive donor polymer for efficient indoor organic Photovoltaics. *Nano Energy*. 2019;58:466-475.
82. Speller EM, Clarke AJ, Luke J, et al. From fullerene acceptors to non-fullerene acceptors: prospects and challenges in the stability of organic solar cells. *J Mater Chem A*. 2019;7(41):23361-23377.
83. Cnops K, Rand BP, Cheyngs D, Verreert B, Empl MA, Heremans P. 8.4% efficient fullerene-free organic solar cells exploiting long-range exciton energy transfer. *Nat Commun*. 2014;5(1):3406.
84. Azzouzi M, Kirchartz T, Nelson J. Factors controlling open-circuit voltage losses in organic solar cells. *Trends Chem*. 2019;1(1):49-62.
85. Bao Q, Liu X, Braun S, Fahlman M. Oxygen- and water-based degradation in [6,6]-phenyl-C₆₁-butyric acid methyl ester (PCBM) films. *Adv Energy Mater*. 2014;4(6):1301272.
86. Florence TM, Lilley SG, Stauber JL. Skin absorption of lead. *Lancet*. 1988;332(8603):157-158.
87. Babayigit A, Ethirajan A, Muller M, Conings B. Toxicity of organometal halide perovskite solar cells. *Nat Mater*. 2016;15(3):247-251.
88. Shi L, Bucknall MP, Young TL, et al. Gas chromatography-mass spectrometry analyses of encapsulated stable perovskite solar cells. *Science*. 2020;368(6497):2412.
89. Li X, Zhang F, He H, Berry JJ, Zhu K, Xu T. On-device lead sequestration for perovskite solar cells. *Nature*. 2020;578(7796):555-558.

AUTHOR BIOGRAPHIES



Benxuan Li is currently a PhD student in the Engineering Department at the University of Cambridge. His research mainly focuses on the organic solar cells, quantum dot-based hybrid solar cells, and other organic optoelectronic devices.



Bo Hou is a Lecturer in the School of Physics and Astronomy, at the Cardiff University. He received his PhD degree from the University of Bristol (2010–2014). He worked as a postdoctoral researcher at the University of Oxford (2014–2018, Wolfson College) and a Senior Research Fellow at the University of Cambridge (2018–2020, St Edmund's College). His research interests include QD synthesis, QD optoelectronics, electron microscopy (TEM), and dynamic charge transfer analysis.



Gehan Amaratunga, FEng., FIET, FRSA, FNASSL, CEng., has held the 1966 Professorship in Engineering at the University of Cambridge since 1998. He heads the Electronics, Power and Energy Conversion Group, one of four major research groups within the Electrical Engineering Division of the Cambridge Engineering Faculty. Professor Amaratunga was elected a Fellow of the Royal Academy of Engineering in 2004. Research in his laboratory includes organic solar cells, inorganic thin-film solar cells, electrochemical and dielectric ultra-capacitors, and solar power systems. He is a Fellow of Churchill College, Cambridge.

How to cite this article: Li B, Hou B, Amaratunga GAJ. Indoor photovoltaics, *The Next Big Trend* in solution-processed solar cells. *InfoMat*. 2021;1–15. <https://doi.org/10.1002/inf2.12180>